ENCIT 2018

ABCM Associação Brasileira de Engenharia e Ciências Mecânicas

17th Brazilian Congress of Thermal Sciences and Engineering
November 25th-28th, 2018, Águas de Lindóia, SP, Brazil

ENCIT-2018-0391
Sizing procedure of a scroll expander prototype for ORC applications

Sabrina Bellé
Paulo Eduardo Batista de Mello
Centro Universitário FEI, Av. Humberto de Alencar Castelo Branco, 3972, São Bernardo do Campo, SP, Brazil, CEP 09850-901
sbelle.eng@gmail.com; pmello@fei.edu.br

Abstract. *Compressed air energy storage (CAES) and organic Rankine cycle (ORC) are promising new technologies that demand scroll expanders with high isentropic efficiency. These devices are a good expander choice for the lower power range, below 10 kW. Internal leakages are the main factor influencing the efficiency of the scroll expander. This work presents considerations about sizing one scroll expander to work with R245fa fluid. The sizing procedure starts with one analysis of the ORC cycle where the expanding device will be used: inlet and outlet pressure, power and mass flow rate. The relation between this operational conditions and the geometry of the expander is discussed.*

Keywords: *Scroll expander, CAES, ORC, internal leakage, isentropic efficiency*

1. INTRODUCTION

Energy storage has gained importance considering the intermittency associated with renewable energy sources, as solar and wind. Jannelli *et al.* (2014) states that reversible hydroelectric power stations and CAES (compressed air energy storage) are the most viable options for energy storage in large scale. According to Sun *et al.* (2015) and Iglesias and Favrat (2014), CAES is also viable for medium and small scales to deal with the intermittency issue of renewable energy sources. For small scale CAES implementation, Mendoza *et al.* (2017), Iglesias and Favrat (2014) and Sun *et al.* (2015) consider the use of scroll expanders a good option.

Declaye *et al.* (2013) converted one oil-free scroll air compressor to operate as an expander in ORC. The working fluid used was R245fa and inlet pressure 12 bar. It was necessary to locate the device inside one hermetic cylinder to avoid fluid leakage. Magnetic couplers were also used. Maximum isentropic efficiency and shaft power produced by the expander were 75.5% e 2.1 kW respectively.

Mendoza *et al.* (2014) used one scroll compressor commonly used in vehicle air conditioning systems and converted the device to be used as an expander. The volumetric ratio of the compressor was 1.9. The authors conducted tests with the expander with air and ammonia. The maximum isentropic efficiency and power measured experimentally were 61% and 958W using ammonia.

The increasing demand for high efficiency scroll expanders have motivated a great number of recent research that consider the thermodynamic behavior of these devices. Most of these researches present experimental tests with compressors converted to expanders. The simulation with CFD (computational fluid dynamics) started to produce useful results more recently. A good review about the subject is presented by Song *et al.* (2015).

Oliveira *et al.* (2017) used transient CFD simulations to study one scroll expander, including the internal leakages. Their results showed that internal leakages modifies the optimum pressure ratio for each maximum efficiency. The maximum efficiency is directly related to volume ratio, but intense internal leakage reduce the pressure ratio for each the maximum is observed. The differences observed through experiments comparison are attributed to friction in the prototype, that was not quantified experimentally.

This work present the sizing procedure necessary to construct one scroll expander prototype to be used in ORC. The prototype will use R245fa as working fluid and is based in the first prototype constructed by the research group (Fanti *et al.* (2016)). Based on the tests conducted with the first prototype is possible to affirm that the sealing system is highly important to achieve a good efficiency. Therefore, modifications in sealing are suggested based in this first prototype.

2. GEOMETRY

The equations used to define the scroll curves are presented by Blunier *et al.* (2009). In the present work, the same equations were used to obtain the scroll curves. The orbital radius that characterize the orbiting scroll motion is also determined by this equations.

Blunier *et al.* (2009) use the involute of circle to define the scroll curves. The radius of the base circle is r_b. Equations 1 and 2 define one orthogonal plane.

$$\mathbf{t}(\varphi) = (cos\varphi, sen\varphi) \tag{1}$$

$$\mathbf{n}(\varphi) = (-sen\varphi, cos\varphi) \tag{2}$$

where $\mathbf{t}(\varphi)$ is the tangent vector and $\mathbf{n}(\varphi)$ the normal vector.

Equations 3 and 4 define the internal and external walls of the fixed scroll, respectively.

$$\mathbf{S}_{fe}(\varphi) = r_b\mathbf{t}(\varphi) - r_b(\varphi - \varphi_{e0})\mathbf{n}(\varphi) \quad \forall\varphi\epsilon\mathbf{I}_e = [\varphi_{es}, \varphi_{max}] \tag{3}$$

$$\mathbf{S}_{fi}(\varphi) = r_b\mathbf{t}(\varphi) - r_b(\varphi - \varphi_{i0})\mathbf{n}(\varphi) \quad \forall\varphi\epsilon\mathbf{I}_i = [\varphi_{es}, \varphi_{max}] \tag{4}$$

The scroll wall thickness e is given by equation 5.

$$e = r_b\left(\varphi_{i0} - \varphi_{e0}\right) \tag{5}$$

The geometry of orbiting scroll walls are defined in a similar way by Blunier *et al.* (2009), with a 180° phase. The orbiting angle θ defines the relative position between the two walls. Equations 6 and 7 define the internal and external scroll orbiting scroll walls respectively.

$$\mathbf{S}_{me}(\varphi) = \mathbf{S}_{fe}(\varphi) - r_o\mathbf{n}(\theta) \quad \forall\varphi\epsilon\mathbf{I}_e = [\varphi_{es}, \varphi_{max}] \tag{6}$$

$$\mathbf{S}_{mi}(\varphi) = \mathbf{S}_{fi}(\varphi) - r_o\mathbf{n}(\theta) \quad \forall\varphi\epsilon\mathbf{I}_i = [\varphi_{is}, \varphi_{max}] \tag{7}$$

The nominal orbiting radius of the expander r_o is given by equation 8. The difference between nominal orbiting radius and real orbiting radius define the tangential gap between scrolls. This gap should be as low as possible to reduce internal leakage.

$$r_o = r_b(\varphi_{e0} - \varphi_{i0} + \pi) \tag{8}$$

2.1 Internal gaps and leakages

The pressure difference between the scroll chambers is sufficiently high to produce leakage between them. This leakage occurs through the gaps, between scroll (flank leakage) walls and on the top of the scroll walls (radial leakage). According to Fukuta *et al.* (2014), sealing is included in the top of the scroll walls to reduce radial leakage. The material used for the sealing should provide small friction coefficient.

Aoun and Clodic (2008) evaluated the performance of one scroll expander with dry water vapor. A special experimental setup was constructed to test the expander. The experimental tests were conducted with two different seals, showing 20% increase in efficiency when a PTFE seal is used. The authors attributed the difference in performance to internal leakage reduction promoted by the sealing.

3. THERMODYNAMIC ANALYSIS

First law analysis is presented for the ORC cycle in many previous works (Zhou *et al.* (2013), Blunier *et al.* (2009), Iglesias and Favrat (2014) and Chang *et al.* (2015)). We use a similar approach to determine the working conditions for the expander.

3.1 Working conditions

A proper design of a scroll expander starts with the definition of volume ratio and volumetric displacement. These two parameters are essential to start the interactive process of defining the variables. The variables define the geometry of the walls presented in the last section: radius of the involute basic circle r_b, initial and final angles ϕ_0 and ϕ_{max}.

The volume ratio of the expander is directly related to pressure ratio. Considerations about the ORC pressure ratio under working conditions are necessary to design an efficient scroll expander. Figure 1 shows the T-s diagram for the ORC considered in the following analysis.

Power demanded by the pump is defined by 9:

$$\dot{W}_P = \dot{m}\left(h_2 - h_1\right) \tag{9}$$

where $\dot{W}_P$ is the pump power, $\dot{m}$ is the mass flow, h_2 the enthalpy at pump outlet and h_1 at the pump inlet. Heat input rate $\dot{Q}_{in}$ in the evaporator is given by 10:

$$Q_{in} = \dot{m}\left(h_3 - h_2\right) \tag{10}$$

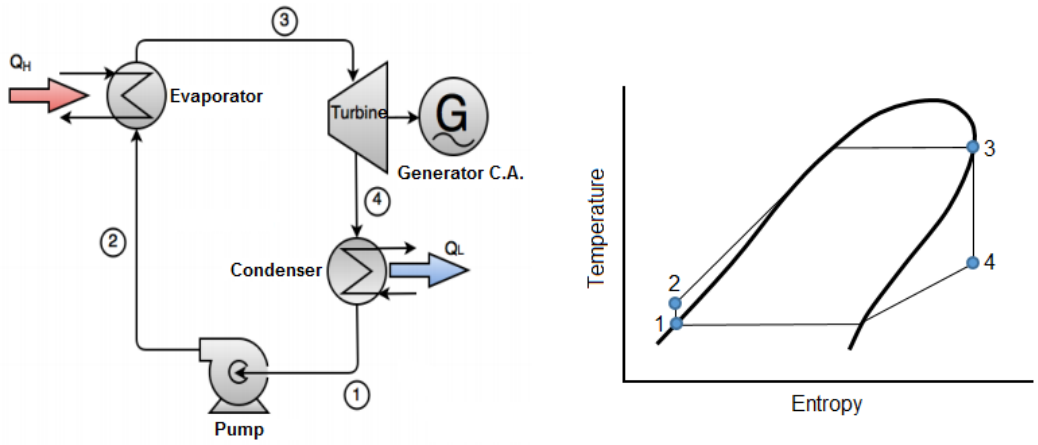

Figure 1. T-s diagram for the ORC analysis

where h_3 is the enthalpy at evaporator outlet.

The power produced by the expander is given by 11:

$$\dot{W}_T = \dot{m}\,(h_3 - h_4) \tag{11}$$

where $\dot{W}_T$ is the power produced and h_4 the enthalpy at expander outlet.

Heat output rate in the condenser is given by 12:

$$Q_c = \dot{m}\,(h_4 - h_1) \tag{12}$$

Thermal efficiency of the cycle is defined by 13:

$$\eta_t = \frac{\dot{W}_T - \dot{W}_P}{Q_{in}} \tag{13}$$

Pressure ratio under working conditions depend on thermodynamic states 3 and 4, as shown in figure 1. The thermodynamic state 4 depends on expander isentropic efficiency.

Volumetric displacement is directly related to mass flow rate, but some estimate of leakages is necessary to consider the unavoidable internal leakages. Mass flow rate is related to power by equation 11. It is necessary to estimate internal leakage $\dot{m}_{leak}$ since it is a considerable part of total mass flow rate $\dot{m}$. Equation 14 presents the relation between mass flow rate and volumetric displacement.

$$\dot{m} = \dot{m}_{in} + \dot{m}_{leak} = \frac{V_{s,exp}\,N}{v_{su,2}} + \dot{m}_{leak} \tag{14}$$

where $\dot{m}_{in}$ is the ideal mass flow rate (without leakages), $V_{s,exp}$ is the volumetric displacement and N the rotational speed.

Previous information about the filling factor is needed to a realistic estimate of the leakage mass flow rate, as shown in equation 15. It is known that filling factor depends on rotation speed and tends to infinity when rotation tends to zero.

$$\phi = \frac{\dot{m}\,\dot{v}_{su}}{\dot{V}_s} \tag{15}$$

where ϕ is the filling factor and v_{su} is the specific volume at expander inlet.

4. RESULTS

The modeling for the ORC characterization was implemented using EES with the objective to verify the influence of evaporation and condensation temperatures over the cycle efficiency, pressure ratio and mass flow rate. For this, some parameters were imposed: pump isentropic efficiency 70%; expected expander isentropic efficiency 65%; rotation speed 2000 rpm and desired power produced by the expander 1.5 kW. The value used for the expander isentropic efficiency is based in indications from the literature.

The results shown in table 1 were obtained for condensation temperature equal to 35°C and evaporation temperature between 80 and 125°C. This condensation temperature could be maintained with a fin and tube heat exchanger, commonly used in air conditioning devices. In this case, condenser heat would be rejected to atmospheric air at ambient conditions.

Table 1. Results for constant condensation temperature T_{cond}=35°C and expander power 1.5 kW.

T_{evap} (°C)	P_{evap} (bar)	$\dot{Q}_{evap}$ (kW)	r_p	r_v	$\dot{m}$ (kg/s)	V_{su} (cm^3/rev)	η_{Carnot}	η_t
80	7.91	20.57	3.75	3.95	0.0956	64.97	0.1274	0.0699
85	8.95	19.03	4.24	4.53	0.0871	52.08	0.1396	0.0754
90	10.09	17.78	4.78	5.18	0.0803	42.26	0.1515	0.0804
95	11.34	16.74	5.37	5.91	0.0746	34.65	0.1630	0.0851
100	12.69	15.87	6.02	6.73	0.0699	28.66	0.1742	0.0894
105	14.16	15.13	6.71	7.65	0.0658	23.87	0.1851	0.0934
110	15.74	14.50	7.46	8.69	0.0624	20.01	0.1957	0.0971
115	17.45	13.94	8.27	9.88	0.0594	16.86	0.2061	0.1005
120	19.29	13.46	9.14	11.23	0.0569	14.25	0.2162	0.1035
125	21.27	13.04	10.08	12.78	0.0547	12.08	0.2260	0.1063

Table 2. Results for constant condensation temperature T_{cond}=45°C and expander power 1.5 kW.

T_{evap} (°C)	P_{evap} (bar)	$\dot{Q}_{evap}$ (kW)	r_p	r_v	$\dot{m}$ (kg/s)	V_{su} (cm^3/rev)	η_{Carnot}	η_t
80	7.91	25.71	2.69	2.84	0.1274	86.65	0.0991	0.0556
85	8.95	23.16	3.05	3.25	0.1130	67.56	0.1117	0.0615
90	10.09	21.19	3.44	3.72	0.1019	53.63	0.1239	0.0669
95	11.34	19.62	3.86	4.24	0.0930	43.19	0.1358	0.0720
100	12.69	18.34	4.32	4.83	0.0858	35.20	0.1474	0.0767
105	14.16	17.28	4.82	5.49	0.0799	28.97	0.1587	0.0810
110	15.74	16.39	5.36	6.25	0.0749	24.03	0.1696	0.0850
115	17.45	15.63	5.95	7.10	0.0707	20.06	0.1803	0.0886
120	19.29	14.98	6.57	8.08	0.0672	16.83	0.1908	0.0919
125	21.27	14.42	7.25	9.19	0.0641	14.17	0.2009	0.0949

We consider a temperature difference of 10°C between T_{cond} and ambient temperature. The condition considered in table 2 refers to another possible implementation: heat rejected by the condenser could be used to heat water. In this case, condensing temperature should be increased.

As expected, the thermal efficiency of the cycle increases for higher evaporation temperature. However, for a proper design of the scroll expander, other parameters should be carefully considered. Data presented in tables 1 and 2 are compared graphically in figure 2.

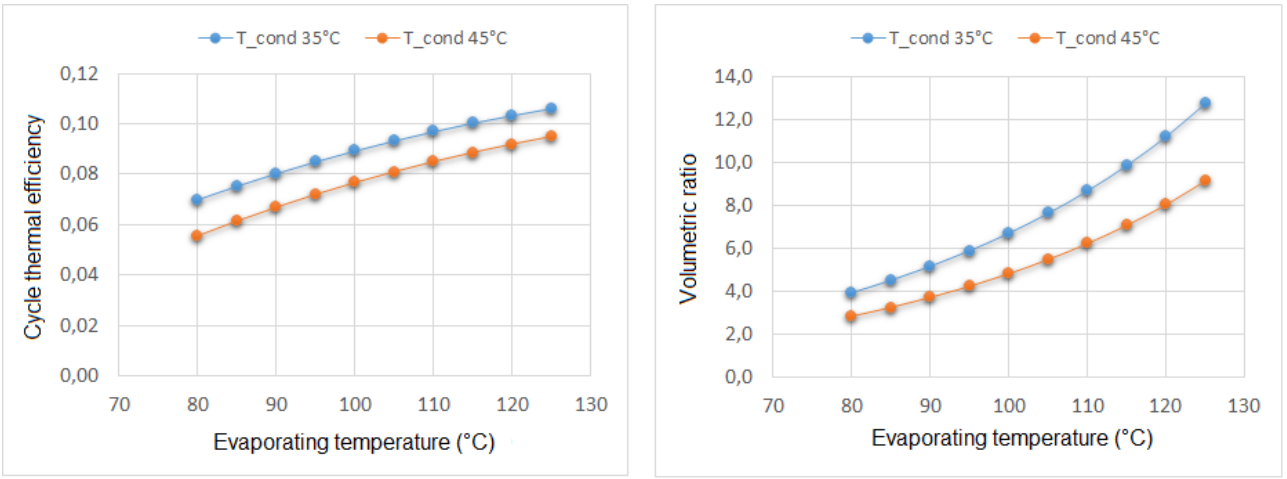

Figure 2. Cycle efficiency (left) and volumetric ratio (right) as a function of evaporation and condensation temperatures.

In figure 2 is possible to verify that optimum volumetric ratio becomes higher as evaporation temperature increase and condensation temperature decreases, the same conditions that leads to a more efficient cycle. As a result, a more efficient cycle requires ideally a higher volumetric ratio expanding device. However, the machine becomes bigger as volumetric ratio increases.

As shown in figure 3, that combines de results shown in figure 2, the ORC efficiency is directly related to volumetric

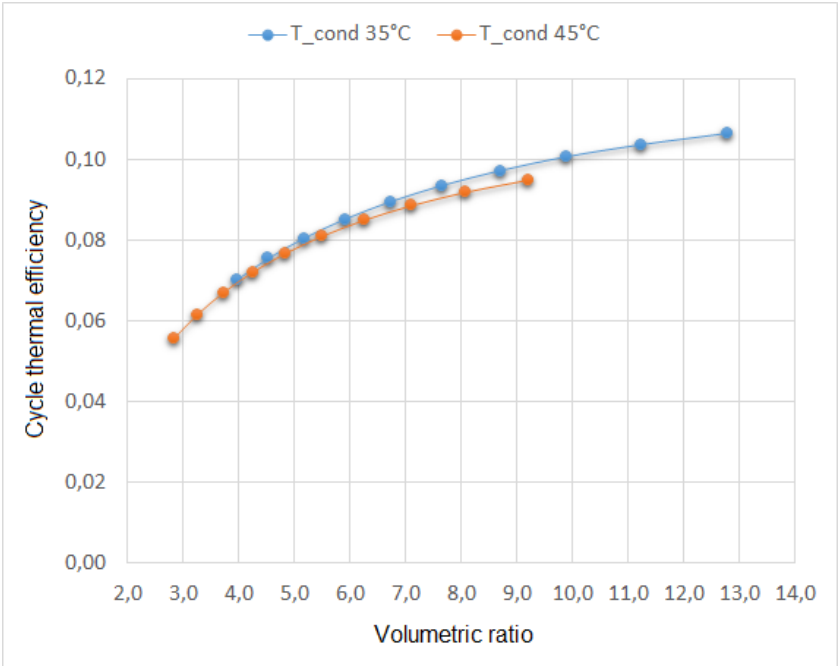

Figure 3. Thermal efficiency of the cycle as a function of volumetric ratio.

ratio. It is possible to use a lower than optimum volumetric ratio expander, but this condition results in small losses associated with under expansion, decreasing the isentropic efficiency of the expander. As a result, there is a compromise between expander size and its isentropic efficiency.

The volumetric ratio of the expander and the length of the scroll curve are related to the geometrical parameter φ_{max} that appears in equations 6 and 7. Figure 4 shows three scroll curve pairs. The volumetric ratio is given by the ratio of volumes shown in blue (discharge chamber) and red (suction chamber). Clearly, the blue volume (discharge chamber) becomes higher when the length of the scroll curve increases, with the undesired increase in machine size.

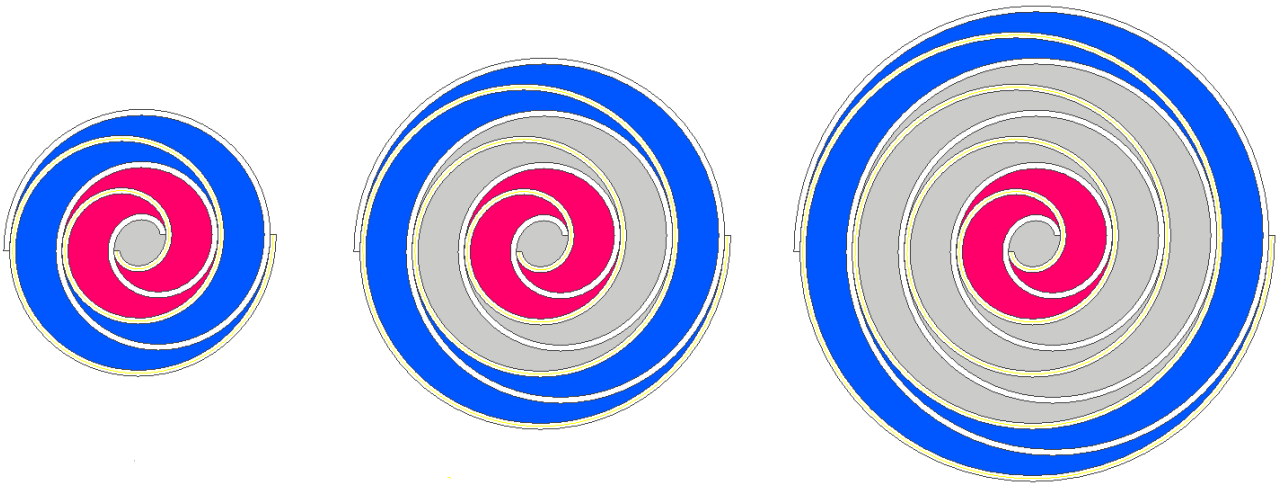

Figure 4. Influence of φ_{max} parameter over the length of the scroll curve and volumetric ratio. When φ_{es} and φ_{is} are equal to $\pi/2$, from left to right φ_{max} = 11/(2π) and r_v = 2; φ_{max} = 15/(2π) and r_v = 3; φ_{max} = 17/(2π) and r_v = 4

.

The chamber volumes can be calculated precisely with a CAD program. For non integer volumetric ratios, as shown in figure 5 for r_v=3.5, this calculation requires repositioning of the orbiting scroll curve, modifying the θ angle.

The height of the scroll walls (in the perpendicular direction of figures 4 and 5) directly increase the volume of the suction and discharge chambers. However, the increases in this height also increase wall deformation due to pressure around the walls and has some negative effect over internal leakages.

Table 3 presents the variation in the wall height and base circle radius r_b simultaneously in order to maintain the volume of suction chamber constant V_{su} = 20 cm^3/rev, and volumetric flow rate as a consequence. As an example, for

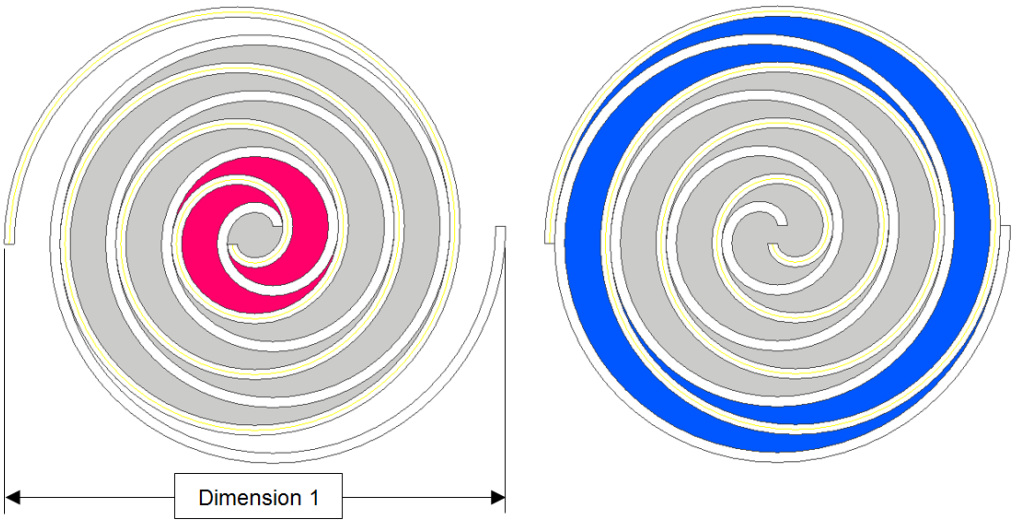

Figure 5. Suction and discharge chambers for volume ratio r_v = 3.5.

volumetric ratio equal to 3,5, the dimension shown in figure 5 increases when the wall height decreases. It reveals another efficiency compromise between expander size and efficiency, in this case due to internal losses.

Table 3. Parameters that result in constant V_{su} equal to 20 cm^3/rev.

Wall height (mm)	r_b (mm)	dimension 1 (mm)
20	17/(2π)	115.12
25	16/(2π)	143.76
30	15/(2π)	135.45
35	14/(2π)	129.07
40	13/(2π)	123.99

The conflict between the expander size and its efficiency impose a design decision. There is no unique solution for the design of a new expander. In the present work, the objective was to design a second scroll expander prototype, based in the experience gained with a first one, that was designed to work with air (Fanti *et al.* (2016)). The second prototype will present volumetric ratio 3.5, wall height of 30 mm, suction chamber volume of 20 cm^3/rev and will operate with R245fa. The parameters used for the construction of the scroll curves are shown in table 4 and should lead to a compact scroll expander.

The expander should present maximum isentropic efficiency operating with evaporation temperature 87.8 °C and condensation temperature 45°C. For higher evaporation temperatures some isentropic efficiency reduction will be observed due to under-expansion.

Table 4. Parameters that define the geometry of the new prototype.

Parameter	symbol	value
radius of the involute base circle	r_b	15/(2π) mm
orbitation radius	r_o	3.5 mm
wall thickness	e	4 mm
initial angle of the external involute	φ_{e0}	$-e/(2r_b)$
initial angle of internal involute	φ_{i0}	$e/(2r_b)$
external starting angle	φ_{es}	π/2
internal starting angle	φ_{is}	π/2
involute final angle	φ_{max}	17/(2π)

5. CONCLUSION

The methodology for the design of a scroll expander was discussed in the present work. As a result, a series of parameters were determined for the construction of a new expander prototype to operate with R245fa. The expander will

present volumetric ratio 3.5 and produce power close to 1.5 kW, depending on operating conditions.

The decision that led to 3.5 volumetric ratio was made considering compactness of the expander and some isentropic efficiency decrease is expected due to under-expansion. Higher volumetric ratios are needed to obtain higher efficiency but would result in a bigger device.

6. ACKNOWLEDGEMENTS

The authors would like to acknowledge Centro Universitário da FEI and Fundação de Amparo à Pesquisa do Estado de São Paulo (FAPESP, Process No. 2011/17657-7) for the research support.

7. REFERENCES

Aoun, B. and Clodic, D.F., 2008. "Theoretical and experimental study of an oil-free scroll vapor expander". In *Proceedings of the International Compressor Engineering Conference, Indiana, USA*. pp. 1–8.

Blunier, B., Cirrincione, G., Hervé, Y. and Miraoui, A., 2009. "A new analytical and dynamical model of a scroll compressor with experimental validation". *International Journal of Refrigeration*, Vol. 32, No. 5, pp. 874–891.

Chang, J.C., Hung, T.C., He, Y.L. and Zhang, W., 2015. "Experimental study on low-temperature organic rankine cycle utilizing scroll type expander". *Applied Energy*, Vol. 155, pp. 150–159.

Declaye, S., Quoilin, S., Guillaume, L. and Lemort, V., 2013. "Experimental study on an open-drive scroll expander integrated into an orc (organic rankine cycle) system with r245fa as working fluid". *Energy*, Vol. 55, pp. 173–183.

Fanti, G.R., Donato, G.H.B. and de Mello, P.E.B., 2016. "A novel scroll expander for flank leakage investigation: preliminary tests". In *Proceedings of the 29th International Conference on Efficiency, Cost, Optimisation, Simulation and Environmental Impact of Energy System*.

Fukuta, M., Ogi, D., Motozawa, M., Yanagisawa, T. and Iwanami, S., 2014. "Seal mechanism of tip seal in scroll compressor". In *Proceedings of International Compressor Engineering Conference*. p. (Paper 2292).

Iglesias, A. and Favrat, D., 2014. "Innovative isothermal oil-free co-rotating scroll compressor–expander for energy storage with first expander tests". *Energy Conversion and Management*, Vol. 85, pp. 565–572.

Jannelli, E., Minutillo, M., Lubrano Lavadera, A. and Falcucci, G., 2014. "A small-scale caes (compressed air energy storage) system for stand-alone renewable energy power plant for a radio base station: A sizing-design methodology". *Applied Energy*, Vol. 78, No. 15, pp. 313–322.

Mendoza, L.C., Lemofouet, S. and Schiffmann, J., 2017. "Testing and modelling of a novel oil-free co-rotating scroll machine with water injection". *Applied Energy*, Vol. 185, pp. 201—-213.

Mendoza, L.C., Navarro-Esbrí, J., Bruno, J.C., Lemort, V. and Coronas, A., 2014. "Characterization and modeling of a scroll expander with air and ammonia as working fluid". *Applied Thermal Engineering*, Vol. 70, No. 1, pp. 630–640.

Oliveira, F.V.d., Silva, F.M. and Mello, P.E.B.d., 2017. "Pressure ratio influence over the performance of a scroll expander". In *24th ABCM International Congress of Mechanical Engineering*. Curitiba, PR, Brazil, p. 232.

Song, P., Wei, M., Shi, L., Danish, S.N. and Ma, C., 2015. "A review of scroll expander for organic rankine cycle systems". *Applied Thermal Engineering*, Vol. 75, pp. 54–64.

Sun, H., Luo, X. and Wang, J., 2015. "Feasibility study of a hybrid wind turbine system–integration with compressed air energy storage". *Applied Energy*, Vol. 137, No. 1, pp. 617–628.

Zhou, N., Wang, X., Chen, Z. and Wang, Z., 2013. "Experimental study on organic rankine cycle for waste heat recovery from low-temperature flue gas". *Energy*, Vol. 55, pp. 216–225.

8. RESPONSIBILITY NOTICE

The authors are the only responsible for the printed material included in this paper.